World Journal of Materials Science and Technology
2024, Vol. 1, No. 1, pp. 1-9
https://doi.org/10.11648/j.wjmst.20240101.11

Research Article

Effect of Vanadium and Austempering Parameters on the Microstructure and Mechanical Properties of Austempered Ductile Iron (ADI) for Tricycle Crankshaft Applications

Sumaila Ochu Abdulrahman[1,*], Saliu Ojo Seidu[2], Akinlabi Abdulwakili Oyetunji[2]

[1]Engineering Research Development and Production Department, Projects Development Institute (PRODA), Enugu, Nigeria

[2]Metallurgical and Materials Engineering Department, Federal University of Technology Akure (FUTA), Akure, Nigeria

Abstract

This research focused on the excellent mechanical properties of austempered ductile iron (ADI) which have been harden to significantly increase its application in the production of automobile parts, and improve their performance. ADI has been produced in this work to replace forged steel crankshaft taking advantage of the significant savings in energy, and the resulting advancement of lightweight and durable material. The suitability of calcined periwinkle ash, as an alternative to ferrosilicon-magnesium, as a nodularizer in ductile iron treatment, was investigated. Varied compositions of calcined periwinkle at 600°C, were used in the treatment of different chemical compositions of molten metal. Response surface methodology – Version 17 of the MINITAB two-level full fractional design 2k-1 + 2k+6 giving 30 research runs (castings) was employed in this study. Also, Molybdenum, Vanadium, Copper, and calcined periwinkle ash as alloying additives at various concentrations was considered. Results show that the 5.5wt.% calcined periwinkle ash that produces good graphite nodules and high nodularity in sample N comprising 3.58% C, 2.60% Si, 0.27% Mn, 0.027% Cr, 0.0098% S, 0.023% P, 0.3% Cu, 0.3% V and 0.2% Mo provided the best mechanical properties. The values obtained were within limits obtained by previous researchers in accordance with the American Society for Testing and Materials (ASTM) A897 130-90-09 standards.

Keywords

Austempered, Nodularity, Molten Metal, Casting, Alloys

1. Introduction

Graphite structure in cast iron gives varied output such as grey cast iron, white cast iron, ductile cast iron, malleable cast iron, and so on. However, when magnesium is added into molten cast iron, it results in to nodular graphite structure in the iron, this is called nodular cast iron, spheroidal graphite cast iron or ductile iron [1]. Steel usually make a rough looking casting and it reduces in size substantially due to solidification shrinkage (2 to 3%) and thermal contraction, as the casting cools to room temperature. The difficulty to control carbon in cast steels also has been a setback, since its strength is primarily a function of the carbon content [2].

The alternative material is undoubtedly austempered duc-

*Corresponding author: sumailaochu@gmail.com (Sumaila Ochu Abdulrahman)

Received: 4 November 2024; **Accepted:** 28 November 2024; **Published:** 19 December 2024

tile iron (ADI). The need to produce engine parts for vehicle and industrial machines within the Nigerian context is long overdue, this becomes more germane considering the economics of importation of such parts. ADI offers cost effective advantages over steel fabrication and forgings [3]. Design flexibility, and versatility have motivated the automobile industries to adopt casting as a better alternative process for manufacturing most of their engine component [4]. However, in substituting forging with casting process for crankshaft production, the restrictive limitation here is the poor casting properties of the conventional materials (steel). Also, ideally, cast crankshaft should be able to handle loads from all dimensions as the grain structure is expected to be uniform and random with the investment casting process [5].

Austempering temperature are in range of 230 – 450 ℃ according to the properties required in the casting's application. At higher austempering temperature (upper bainitic range), the ferrite nucleates and grows into austenite [6]. Lower austempering temperatures produce finer and greater volume fraction of ferrite and higher yield strength. The nature of ausferrite microstructure depends not only on austempering temperature but a lower volume fraction of ferrite which is accompanied by lower yield strength [7]. In this research work, the effect of copper, molybdenum and vanadium alloys as well as the effect of heat treatment parameters such as austempering temperature and austempering time on mechanical properties and microstructure of the ductile iron on the tricycle crankshaft applications were studied.

Studies revealed that conventionally, crankshafts are produced from American Iron and Steel Institute (AISI) 5140 (high carbon steel) by drop forging in dies. This process is however, very expensive because of high initial capital investment, especially in the procurement of the dies. Hence, there is need for an alternative process which will compete with the conventional method at relatively lesser cost. Out of the various metal forming processes existing, casting process has proved to be the best alternative to forging for crankshaft production. Because of its intricate shapes and desired dimension with specified properties that are easily produced directly from molten metal with less expenditure of energy, material and labour.

Also, in Nigeria, transportation by means of tricycle is becoming more popular due to the role this mode of transportation plays in reducing poverty and moving people from one destination to the other; there is an increased number of operators currently in the business in Nigeria. Tricycles are often used for short – distance travelled, especially in areas where motorized vehicles may not be practical or available. The Tricycles can carry passengers, goods, or both, depending on their design and purpose. As a result, other economic activities especially spare parts business and tricycle mechanics begin to thrive as the tricycle crankshaft from time to time get damaged. Nigeria Gross Domestic Product (GDP) would have been greatly enhanced if the volume of tricycle crankshaft importation is reduced drastically through local production of the functional crankshaft thereby creating employment opportunity for Nigerians.

2. Materials and Methods

a. Pig iron, cast iron and steel scraps used in this research were obtained from Coal Camp Market in Enugu State.
b. Perwinkle shell was collected from Nembe in River State.
c. Plaster of Paris otherwise called gypsum were purchased from the open market.

2.1. Production of Mould

The mould was prepared using Plaster of Paris (POP) otherwise called gypsum and water. Both the gypsum and water were measured by weight and expressed in numerical ratio and the equation expressed in terms of 100 parts of plaster. The mixture was in proportion of 100 parts of gypsum added to 67 parts of water and stirred slowly to creamy consistency. The mixture was then poured into the mould boxes where the split pattern of the tricycle crankshaft was positioned. After the setting of the mould at 3 minutes, the pattern was removed from the mould thereby created cavity in the mould.

2.2. Charge Materials Preparation

The raw materials for melting were cleaned with hard wire brush to remove the sand and oil from the scraps. The prepared charged materials were placed inside tilting graphite crucible furnace already superheated at a temperature of 1430°C to melt the materials. At this pouring temperature, the molten metal was tapped from the furnace into the treated ladle with calcined periwinkle ash as nodularizer covered with steel plate to prevent the nodularizer from floating, this method is known as sandwich method. Meanwhile the inoculation was carried out using ferrosilicon along the stream of molten metal to the ladle.

The periwinkle shell collected from Nembe in River State were washed, dried, then calcined at 600 ℃, 800 ℃ and 1000 ℃ for 2 hours in muffle furnace, crushed, and sieved with 0.25 – 1.44mm sieves (75 micron) and its composition were determined by analysis laboratory in PRODA, Enugu using an X-ray fluorescence (XRF) machine (PANalalytical).

In this work, the sample calcined at 600°C was used in treating the molten ductile iron as nodularizer.

3. Results and Discussions

3.1. Experimental Design and Data Analysis Procedure

Evaluation, modelling and optimization using optimization software involved the:

i. Development of appropriate Response Surface Methodology (RSM) experimental plan.
ii. Fitting and selection of the best response surface models.
iii. Optimization of the selected models and
iv. Verification/confirmation of the modeling and optimization results.

The choice of the experimental design was be based on the study objectives, number of variables, resource availability and source of data collection. Effects of the alloying elements on the ductile iron crankshaft investment casting production process; copper plate, vanadium and Ferro-molybdenum on the performance parameters of the ductile iron crankshaft – tensile strength (T_S), wear rate (W_R), fatigue strength (F_S), impact strength (I_S) and hardness strength (H_S) [8].

A two-level full factorial design g (2^k + 2k+6) giving 30 experimental runs was employed in this study because of its economic viability, desirable properties, orthogonality and it permits marginally small experimental runs that was analyzed for high factorial points. Minitab Release 17 software with experimental study variable number (k = 4) for independent variables including; copper plate, Ferromolybdenum (FeMo) and FerroVanadium (FeV) was used for the design and analysis of the results. The factorial design generated from equation 1 to 6 was used to develop a first order model for the Tensile strength (T_S), hardness strength (H_S), impact strength (I_S), fatigue strength (F_S) and wear rate (W_R) of the form.

$$y_m = f(x_1, x_2 ... x_k) + \varepsilon_m \quad (1)$$

Where y represents the responses in their natural units, m is the number of responses in the design (i.e. 3), x represents the factors in their coded forms, k is the number of factors in the design (i.e. 3) and ε is the error (also known as residual) in the design.

$$X = \left(\frac{x - \left(\frac{x_{max} + x_{min}}{2} \right)}{\left(\frac{x_{max} - x_{min}}{2} \right)} \right) \quad (2)$$

$$x_1 = \frac{Cu - 0.3}{0.1} \quad (3)$$

$$x_2 = \frac{FeMo - 0.2}{0.1} \quad (4)$$

$$x_3 = \frac{FeV - 0.8}{0.5} \quad (5)$$

$$x_4 = \frac{CPA - 5.5}{4.5} \quad (6)$$

The responses computed from the results of the factorial runs was used with the coded factor levels to fit the coded linear functions (main effects) of the performance indicators and the operational variables of the tricycle crankshaft production using MINITAB. The search for the models that adequately described the responses fitted the linear function because of the desire to quantify the parameters with the simplest possible functions. However, the main effects plots, model adequacy measures and residual diagnostic plots displayed by the software along with the fitted linear models were used to evaluate if the functions approximate the true responses adequately.

3.2. Casting of the Molten Metal

The chemical composition of the molten metal was confirmed using a spark spectrometer which showed the expected chemical composition before pouring into the ladle, and then to the ceramic shell moulds in the form of solid cylindrical shape of length 280mm and diameter 30mm for specimen analysis and on the crankshaft shell ceramic moulds.

Figure 1. *ADI Crankshaft without In-gates.*

Figure 2. *ADI Crankshaft with In-gates.*

3.3. Heat Treatment Process

The basic production of ADI process consists of two separate and controlled steps – austenitizing and austempering – as seen in figure 3 below.

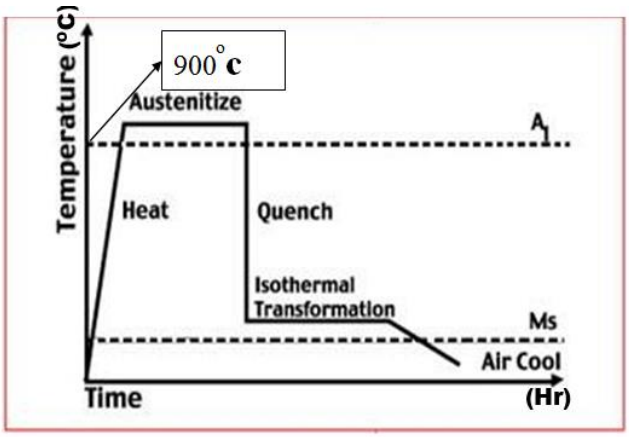

Figure 3. *Heat treatment cycle for the ADI.*

After initial preheating of the samples for 10 minutes at 450 ℃ to remove oil / dirt from the sample surface in a preheating furnace, the samples were heated to temperature of 900 ℃ for 60 minutes in a sealed / enclosed furnace.

The austenitizing temperature and time were selected from the preliminary experiments on the basis of the minimum level required to completely austenitize the entire sample. Then, they were all subjected to austempering, an isothermal heat treatment technique, in which samples were quenched in a molten salt bath of 50%wt sodium nitrate and 50%wt potassium nitrate salts [9].

The transfer of the samples from an elevated temperature to the quench tank was carried out within 5 seconds while the temperature was monitored to ensure isothermal transformation to obtain an ausferrite structure.

The austempering was carried out at a temperature of 300 ℃ for three (3) different times of 30 minutes, 45 minutes and 60 minutes respectively, to study the effect of the austempering time on the mechanical properties and its microstructural evolution. The temperature and times were chosen to avoid the formation of martensite at a lower austempering temperature of 300 ℃. After the austempering process, the samples were fed into the hot water washing machine for 30 minutes to remove salt on the surface of the samples [10].

3.4. Microstructural Preparations

Microstructural examinations of the As – Cast and ADI samples were carried out using an optical microscope Olympus PMG – 3 model at Ahmadu Bello University Zaria, according to ASTM A247 standard. The micrographs were obtained after sequence of metallographic preparations. This involves grinding and polishing with different grades of emery papers and polishing with paste on polishing cloth. The samples were etched using 2% nital solution that revealed the volume fraction of phases and micro constituents.

3.5. Mechanical Testing

Hardness Test

The heat-treated samples were polished separately from As-cast samples for hardness measurement. Rockwell hardness test was performed at room temperature to measure the hardness of the ADI as well as the As-cast sample of ductile cast iron specimens on C-scale. A load of 150 kgf was applied to the specimen for 30 seconds through the square shaped diamond cone indenter for the austempered and that of as-cast samples. Three measurements for each sample were taken, covering the whole surface of the specimen and average of the results were taken to obtain final hardness results.

Tensile Strength Test

Tensile Strength test was carried out according to ASTM (A370-2002). A specimen of "Dog Bone Shape" shown in figure 4 was prepared for tensile test which were machined to 10 mm gauge diameter and 70 mm gauge length. Test was conducted by using universal testing machine (UTM 100) as per ASTM standard.

Impact Tests

Impact tests were conducted using a Charpy type impact tester and the samples for the test were cut from the solid cylindrical shape produced and reshaped into the rectangular form. The unnotched samples were tested on the machine in cold working conditions, in dimensions of 55mm x 10mm x 10mm according to the ASTM specifications.

Wear Test

Wear test was carried out on Anton Paar Tribometer (TRB) machine, that utilizes pin- on – disk having stainless steel indenting ball of radius 5mm. This was done in accordance with ASTM G99 – 05 – 16 standards. Contact load of 8N was applied on all the specimens at a speed of 150 revolutions per minute (rpm) and linear speed of 7.85 cm|s for 30 minutes. For the total time of 30 minutes utilized for the test, sliding distance of 60 m was covered. Volumetric wear rate was estimated in accordance with [11] by measuring the mass loss in each sample after each test.

The initial mass of each sample was first taken and after the wear operation, final mass was taken and loss in mass was calculated which is used to calculate volume loss.

$$\text{Wear volume} = \frac{Wear\ Mass}{Density} \tag{7}$$

$$\text{Specific wear rate} = \frac{Wear\ Volume}{Sliding\ Distance\ x\ Force\ applied} \tag{8}$$

This is in accordance with Agbeleye *et al* (2017).

Wear Resistance of ADI

ADI are widely used in the manufacturing of automobile parts including those parts that mostly experience surface contact when subjected to high pressure and external load, with relative motion. These parts need to show high performance on wear resistance at high temperature and cyclic loading. This is evident to investigate and understand the tribological behaviour of ADI of crankshaft [12].

The wear resistance of ADI happened to decreased while increasing the austempering time as the macro hardness reduced with the formation of more ausferritic structure rather than martensite.

4. Results and Discussions

It is concluded that the ADI have an outstanding wear resistance performance which could be attributed to the high fracture toughness of the unique ausferritic structure of the produced ADI matrix and the induced transformation from retained austenite into martensite to improve the surface hardness as the fracture toughness improved due to carbon saturated austenite.

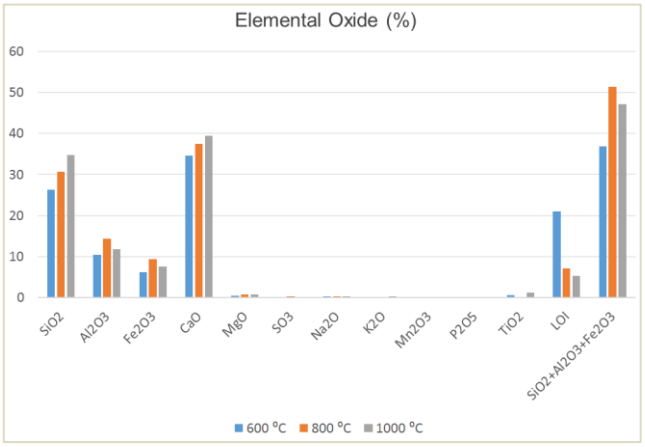

Figure 4. *Chemical Composition of Periwinkle Shell Ash calcined At Different Temperatures.*

4.1. Chemical Composition Analysis of Periwinkle Shell Samples

The major chemical composition is CaO in the periwinkle shell ash and met the required standard and its role is to desulphirize and deoxidize in cast iron and increase the fluidity of the molten metal. In the cast, iron melt with calcium which reacts with oxygen and produces the oxide CaO, which becomes part of the silicate phase and the phase is deposited on the surface of their oxides in the melt and become activated nuclei which accelerate graphite nucleation growth. This means that in order for solidification to take place, the melt has to be relatively little subcooled and prevent the sub-stable solidification from occurring and the generation of iron carbides. The choice of higher temperature for calcination offers a higher value of CaO which leads to poor mechanical properties of the ductile cast iron as a result of carbide formation, thus the choice of 600°C with less value of CaO is evident [13].

4.2. Effect of Austempering Time on Tensile Strength

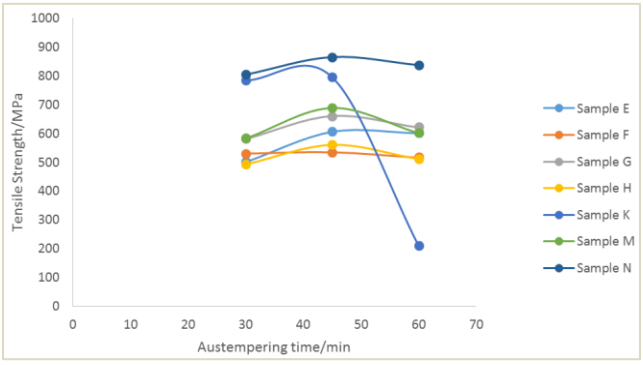

Figure 5. *Variation of tensile strength with respect to the austempering time at a temperature of 300°C.*

Figure 5 revealing the different of tensile strength with respect to the austempering times of 30 minutes, 45 minutes and 60 minutes. It is noticed that the tensile strength is increasing from austempering time of 30 minutes to 45 minutes and start decreasing from 45 minutes to 60 minutes.

As shown in the figure 5, the tensile of ADI decreases with an increase in the austempering time. In stage 1 of isothermal transformations, it is reported that the amount of retained austenite in the samples could be the reason for decrease in the tensile strength of ductile iron with increasing austempering time.

The low austempering time produce finer ferrite needle shaped ausferrite microstructure with a lower amount of retained austenite and graphite nodule, which in turns increased the tensile strength. The addition of copper has resulted in the strengthening of the as-cast ductile iron due to the promotion and refining of the pearlitic phase that significantly increased the tensile strength. But as the time increases, the structure shows coarse acicular ferrite with high amount of retained austenite and graphite nodules resulted to a decrease in tensile strength.

4.3. Effect of Austempering Time on Elongation

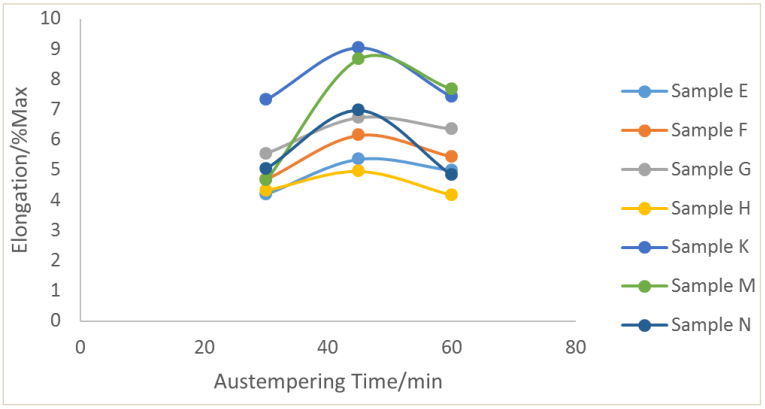

Figure 6. *Variation of elongation with respect to the austempering time at a temperature of 300°C.*

Figure 6 shows the variation of elongation with respect to the austempering time at a temperature of 300°C. the elongation is increasing from 30 minutes to 45 minutes, and from 45 minutes to 60 minutes, it is decreasing. At a low austempering time, the lower elongation values was recorded in the sample which could be attributed to the presence of martensitic in the matrix of the ausferritic structure. But the ductility is found to increase with increasing austempering time up to 45 minutes due to the increased in the amount of retained austenite and less martensitic on subsequent cooling to room temperature. Beyond 45 minutes a decrease in ductility is seen in some samples due to start of the stage II of austempering reaction when retained austenite decomposed to ferrite and carbide.

4.4. Effect of Austempering Time on Hardness

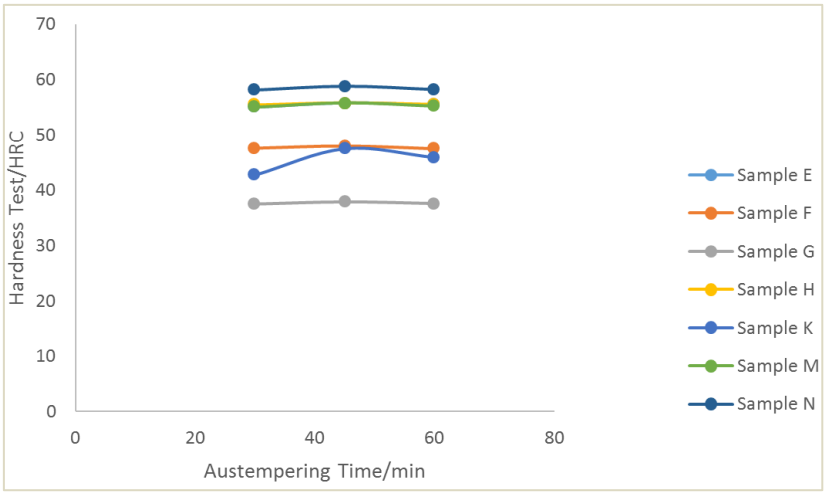

Figure 7. *Variation of hardness with respect to the austempering time at a temperature of 300°C.*

As seen in figure 7, it is observed that during the short time of austempering, the hardness value of the ADI recorded increases as during the subsequent cooling from austempering temperature to room temperature, the martensitic formation cannot be avoided. But with an increase in time, there is an increase in the carbon of the austenite that has resulted in a decrease in M_s and M_f temperatures. At higher austempering time, there is an increase in the amount of retained austenite which results in decrease in hardness. The addition of vanadium to the ductile iron increased the hardness due to the increase in the pearlite amount as it changes the speed of austempering reaction. But at a higher austempering time, the values recorded reduces due to the increased in the amount of carbon that present in austenite.

4.5. Effect of Austempering Time on Fatigue Strength

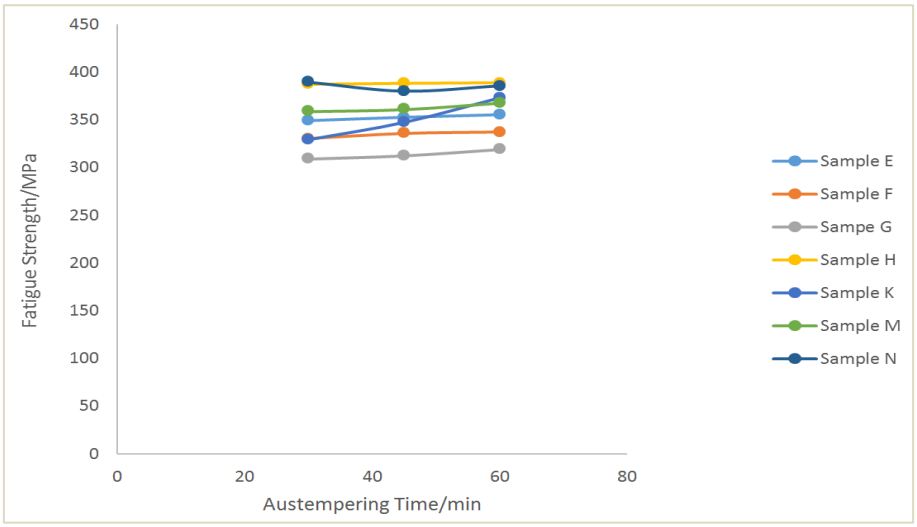

Figure 8. *Variation of Fatigue Strength with respect to the austempering time at a temperature of 300°C.*

At a lower austempering time as shwn in figure 8 above, the fatigue strength values recorded were very low due to the finer acicular ferrite of the sample. However, a higher amount of retained austenite and graphite nodules with coarser acicular ferrite experience at higher austemperting time increased the fatigue strength. This could be attributed to the strain induced transformation of retained austenite into martensitic.

4.6. Effect of Austempering Time on Impact Test

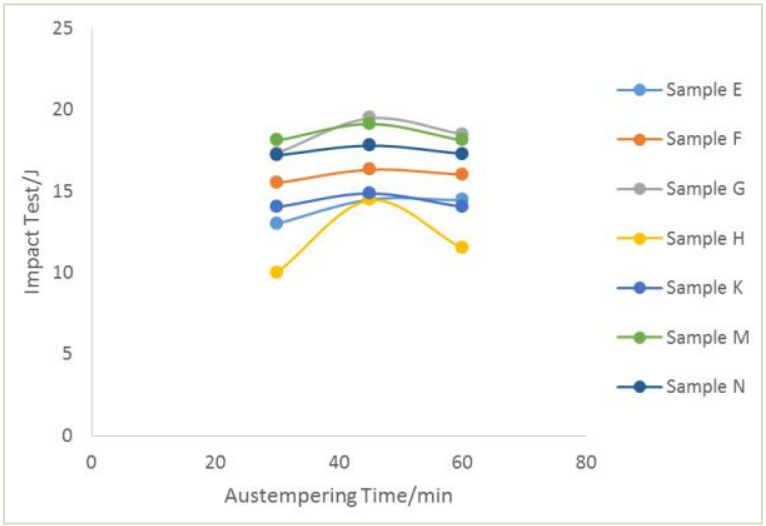

Figure 9. *Variation of Impact Test with respect to the austempering time at a temperature of 300°C.*

It is observed from the graph, as shown in figure 9 above, at lower austempering time of 30miuntes, the ADI sample shows needle shape acicular ferrite containing high amount of austenitic carbon as a result of the presence of calcined periwinkle ash that impedes the motion of dislocation as caused the increase in toughness. But at higher austempering time, it reveals that the sample is of coarse acicular ferrite with high amount of retained austenite and graphite nodules which resulted in decrease of the toughnes.

4.7. Effect of Austempering Time on Wear Rate

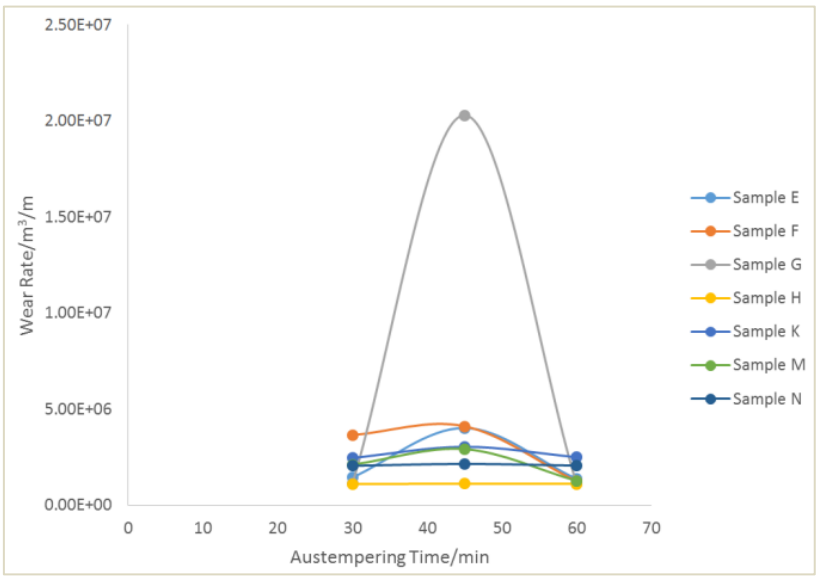

Figure 10. *Variation of wear rate with respect to the austempering time at a temperature of 300°C.*

At a low austempering time from 30 minute to minutes indicated in the graph, it is observed that the wear loss was reduce. This could be due to the fine lower ausferritic microstructure. But as the time increased to 60 minutes the wear loss on the samples were observed to increase as a result of coarse in nature of the sample due to the formation of a greater amount of retained austenite.

The high amount of strain is significantly high, allowing it to have a long service life. The outcomes come from ANSYS test showed that the shear for exerted on the ASTM A536 100 – 70 – 03 (GGG 70) high ductile than material is more as compared to AISI – 4140 alloy steel (EN 19C) before enlistment solidifying. Effect test demonstrated that the weight of AISI – 4140 alloy steel (EN 19C) is 3kg higher than ASTM A536 100 – 70-03 (GGG70) [15] The crankshaft is subjected to different pressure load with respect to crank angle and therefore the study of the crankshaft is subjected to different performance conditions, which is the most significant for an effective design in the internal combustion engines.

5. Conclusion

In conclusion, the findings of this study indicated the following:

1. That the coating of critical points like crankpin and journal of the ceramic shell moulds using the mixed calcined periwinkle ash with refined oil improved the surface quality of casting and enhanced its fatigue strength.
2. That the samples austempered at longer times reveal microstructures with upper acicular structure, and those austempered at shorter times revealed microstructures with lower acicular structure.
3. That the uses of calcined preiwinikle ash as nodularizer increased the presence of graphite in ADI that improved the wear resistance of the crankshaft despite its relative motion during operation in addition to the external load that caused the component exposed to surface contact.
4. That as the austempering time is increased, tensile strength, hardness and elongation increased in the alloyed ADI crankshaft.
5. That the nodular count of ADI produced reveals smaller nodule sizes with increasing austempering time, with a corresponding increase in tensile strength. Fatigue strength and toughness are improving overall, fatigue failure is reduced, and the life span of the crankshaft is prolonged.
6. That the use of vanadium has notable effects on the properties of the heat-treated crankshaft due to its strong affinity for nitrogen that eliminates the aging tendency and cold brittleness, thereby greatly reducing the frequent breakdown of crankshaft.

Abbreviations

ADI	Austempered Ductile Iron (ADI)
PRODA	Projects Development Institute
FUTA	Federal University of Technology, Akure
ASTM	American Society for Testing and Materials
AISI	American Iron and Steel Institute
GDP	Gross Domestic Product

POP	Plaster of Paris
XRF	X-ray Fluorescence
RSM	Response Surface Methodology
T_S	Tensile Strength
W_R	Wear Rate
F_S	Fatigue Strength
I_S	Impact Strength
H_S	Hardness Strength
FeMo	Ferromolybdenum
FeV	FerroVanadium
UTM	Universal Testing Machine
RPM	Revolution Per Minute

Conflicts of Interest

The authors declare no conflicts of interest.

References

[1] Abdullahi, B., Alias, S., Jaffar, A., Rashid, A. and Ramli, A. (2010). Mechanical properties and microstructure analysis of 0.5% niobium alloyed ductile iron on under austempered process in salt bath treatment, *International Conference on Mechanical and Electrical Technology* (ICMET) 610-614.

[2] Kawalec, M., and Kozana, J. (2014). Effect of microstructure of Fe-C-V alloys on selected functional properties, *Archives of Foundry Engineering*, 14, (3): 33-36.

[3] Adewuyi, B. O. (2018). Metals and Materials: Creating Technological Entrepreneural Potentials, Inaugural Lecture Series 94. The Federal University of Technology, Akure. Nigeria. 7-30.

[4] Dakre V, Peshwe D, Pathak S, Likhite A. TEM analysis of austempered ductile iron processed through conventional and two-step austempering process. Trans Ind Inst Met 2019; 72(4): 911e7.

[5] Orlowicz, A. W., Mroz, M., Tupaj, M., and Trytek, A. (2015). Shaping Microstructure of Cast Iron Automobile Cylinder Liners aimed at Providing High Service Properties. *Achieves of Foundry Engineering,* 15 (2): 75-78.

[6] Francesco, L., Vittorio, D. C., and Maurio, C. (2015). Fatigue Crack Propagation in a Ferritic – Pearlitic DCI: Overload Effects on Damaging Mechanism, *Proceedia Engineering*, 109: 35-42.

[7] Heidarian, B., Nilli-Ahmadabadi, M., and Moradi, M. (2010). Mechanical Properties of Thixoformed formed Austempered Ductile Iron. *Transaction of Non Ferrous Metals Society of China* 20, 798- 804. Journal of cleaner production, (140): 1739-1748.

[8] Hegde A, Sharma S, Sadanand R. Mechanical characterization and optimization of heat treatment parameters of manganese alloyed austempered ductile iron. J Mech Eng Sci 2019; 13(1): 4356e67.

[9] Krzynska, A. and Kochanski, A. (2014). Austenitization of Ferritic Ductile Iron, *Archives of Foundry Engineering,* 14(4): 49–54.

[10] Nebojsa, N., Tadic, N., and Jovan, D. (2017). Influence of IC Engine Crankshaft Main Journals Lengths on Main Bearings Load. 315 – 322.

[11] Vijar K. D., Ayyagari, S. and Prasad, M. J. N. V. (2017): Mechanical Characteristics and Electrochemical Behaviour of Electrodeposited Nanocrystalline Iron and Iron-Nickel Alloy, Materials Chemistry and Physics 201, 26 – 34.

[12] Zhang, N., Zhang, J., Lu, L., Zhang, M., Zeng, D. and Song, Q. (2016): Wear and Friction Behavior of Austempered Ductile Iron as Railway Wheel Material. Materials and Design 89. 815- 822.

[13] Chen X, Zhao L, Zhang W, Mohrbacher H, Wang W, Guo A, et al. Effects of niobium alloying on microstructure, toughness and wear resistance of austempered ductile iron. Mater Sci Eng 2019; 760A: 186e94.

[14] ASTM A897/A897M-16. Standard specification for austempered ductile iron castings. West Conshohocken, PA, USA: ASTM International; 2016.

[15] Wang B, Qiu F, Barber G, Pan Y, Cui W, Wang R. Microstructure, wear behavior and surfacehardening of austempered ductile iron. j mater res technol 2020; 9(5): 9838e55.